JOURNAL OF MATERIALS SCIENCE: MATERIALS IN MEDICINE **16** (2005) 977–983

Age-hardening behaviour and microstructure of a silver alloy with high Cu content for dental application

HYO-JOUNG SEOL[1], YOUNG-GU PARK[1], YONG HOON KWON[1], YUKYO TAKADA[2], HYUNG-IL KIM[1,*]
[1]*Department of Dental Materials, College of Dentistry, Pusan National University, 1-10 Ami-dong, Seo-gu, Pusan 602-739, South Korea*
[2]*Division of Dental Biomaterials, Graduate School of Dentistry, Tohoku University, 4-1 Seiryo-machi, Aoba-ku, Sendai 980-8575, Japan*

Age-hardening behaviour and the related microstructural changes of a silver alloy with relatively high Cu content were elucidated by means of hardness test, X-ray diffraction (XRD), scanning electron microscopic (SEM) observations and electron probe microanalysis (EPMA). The microstructure of the solution-treated specimen was composed of the Ag-rich matrix, the Cu-rich particle-like structures containing Pd, and the lamellar structure of both phases. By the age-hardening heat-treatment, the Cu element began to precipitate from the Ag-rich matrix by the solubility limit, and the very fine Cu-rich precipitates became coarsened by further aging. The silver alloy with relatively high Cu content showed apparent age-hardenability. The hardness of the solution-treated specimen began to increase and reached a maximum value with increasing aging time, and then the hardness decreased gradually after maintaining the maximum value for short periods of time. The early stage of precipitation of the Cu-rich phase from the Ag-rich matrix seemed to have caused the increase in hardness. The decrease in hardness was attributed to the coarsening of the Cu-rich precipitates in the later stage of the age-hardening process.

1. Introduction

The microstructure of dental casting alloys depends greatly on the alloy composition, and can be changed by age-hardening heat treatment which is required for the dental casting alloys that belong to type III and IV to obtain proper mechanical property. The dental casting alloys of type III and IV are designed to have apparent age-hardenability by the age-hardening heat treatment. A usual hardening element for dental gold alloys and silver alloys is known as Cu, and the atomic ratio of Cu to Au or Ag determines the age-hardenability and hardening mechanism [1–4]. However, Cu is prone to tarnish and corrosion. Thus, the Cu content must be adjusted to satisfy both the age-hardenability and chemical stability of the dental alloys. From the viewpoint of chemical stability, microstructural homogeneity is preferred because the alloy of complex microstructures is easy to be preferentially corroded on the less noble phase. Therefore, the chemical stability of Cu-containing dental alloys can be improved if the Cu element forms the single phase with other chemically stable elements.

Dental silver alloys for the crown and bridge fabrication are generally composed of more than 50 wt% of Ag and approximately 30 wt% of Pd and Au, and the Cu content for these alloys is usually less than 10 wt%. The age-hardening characteristics and microstructure of dental silver alloys have been studied several times [4–6], and it was revealed that the Cu content has a great effect on the age-hardenability and microstructure of the dental silver alloys. Therefore, if the Cu content in silver alloys is relatively high, the age-hardenability and microstructure of the alloys can be changed. However, there are few studies on the dental silver alloys with relatively high Cu content, and its age-hardenability and microstructural changes during age-hardening is not clear.

In the present study, the dental silver alloy composed of 50 wt% Ag −20 wt% Cu −20 wt% Pd −10 wt% Au was used for the purpose to elucidate the age-hardening behaviour and related microstructural changes of the dental silver alloy with relatively high Cu content by means of hardness test, X-ray diffraction (XRD), scanning electron microscopic

*Author to whom correspondence should be addressed.

TABLE I Chemical composition of the alloy used

Composition	Ag	Cu	Pd	Au
at.%	45.58	30.95	18.48	4.99
wt.%	50	20	20	10

(SEM) observations and electron probe microanalysis (EPMA).

2. Materials and methods

2.1. Chemical composition of the alloy

The chemical composition of the alloy is 50 wt% Ag −20 wt% Cu −20 wt% Pd −10 wt% Au as listed in Table. I. To prepare the specimen alloy of above composition, plates or shots of more than 99.95 wt% for each element were mixed and melted three times, and then rolled. After that, the rolled alloy sheets were cut into small pieces, and melted over four times to avoid segregation. Then, they were rolled to plate-like shape of 1.5 mm thickness. Final weight loss of alloy is less than 0.03 % of the weight before melting.

2.2. Hardness test

Before the hardness test, above-mentioned plate-like specimens were solution- treated at 750 °C for 30 min under an argon atmosphere, then rapidly quenched into ice brine not to allow for equilibrium to occur. Then, they were isochronally aged in the temperature ranges of 300 to 550 °C, and were isothermally aged at 350 and 400 °C for various periods of time in a molten salt bath (25% KNO_3 + 30% KNO_2 + 25% $NaNO_3$ + 20% $NaNO_2$) which was used for the temperature range from 150 to 550 °C, then quenched into ice brine for hardness test.

Hardness measurements were made using a Vickers micro-hardness tester (MVK-H1, Akashi Co., Japan) with a load of 300 gf and dwell time of 10 s. Vickers hardness results were obtained as the average values of five measurements.

2.3. X-ray diffraction study

For the XRD study, powder specimens that passed through a 330-mesh screen were obtained by filing the plate-like samples. After being vacuum-sealed in a silica tube and solution-treated at 750°C for 30 min, they were isothermally aged at 400°C for various periods of time in a molten salt bath, and then quenched into ice brine. The XRD profiles were recorded by an X-ray diffractometer (XPERT-PRO, PHILIPS, Netherlands). The X-ray diffractometer was operated at 30 kV and 40 mA, and Nickel-filtered CuKα radiation was used as the incident beam.

2.4. Scanning electron microscopic observations and electron probe microanalysis

For the SEM observations, the plate-like samples were subjected to the required heat treatment, and then they were prepared by utilizing a standard metallographic technique. A freshly prepared aqueous solution of 10% potassium cyanide and 10% ammonium persulfate was utilized for the final etching of the samples. The specimens were examined at 20 kV using a scanning electron microscope (S-2400, Hitachi, Japan).

EPMA was made on the plate-like specimens used for the SEM observations. The specimens were examined at 15 kV using an electron probe X-ray microanalyser (EPMA–1600, Shimadzu, Japan).

3. Results and discussion

3.1. Age-hardening behaviour

Fig. 1 shows the isochronal age-hardening curves of the specimen alloys solution-treated at 750 °C for 30 min and then aged in the temperature ranges of 300 to 550 °C for 10 and 20 min. Age-hardening behaviour of the specimen alloys aged for 10 and 20 min showed a similar tendency in the temperature ranges of 300 to 550 °C. The specimen alloy solution-treated at 750 °C for 30 min showed apparent age-hardenability at the aging temperatures of 350 and 400 °C. Thus, the isothermal age-hardening curves were obtained at those aging temperatures to evaluate the age-hardenability of the specimen alloy.

Fig. 2 shows the age-hardening curves of the specimen alloys aged isothermally at 350 and 400 °C. The isothermal age-hardening curves at 350 and 400 °C displayed a similar tendency, but the increasing and decreasing rates in hardness at 400 °C were slightly faster compared to those at 350 °C. This must result from the fact that the diffusion occurs faster at the higher temperature. The hardness of the solution-treated specimen began to increase and reached a maximum value with increasing aging time, and then the hardness decreased gradually after maintaining the maximum value for short periods of time. Considering the similarity in the age-hardening behaviours at 350 and 400 °C, the age-hardening at these temperature ranges was supposed to undergo the same mechanism.

3.2. XRD study

Variations of XRD pattern during the isothermal aging were examined to clarify the age-hardening mechanism of the specimen alloy. Fig. 3 is showing XRD changes during isothermal aging at 400 °C with aging time. The XRD pattern of the solution-treated specimen at 750 °C for 30 min shows two phases, α_1 and α_2 of a face-centered cubic (f.c.c.) structure with a lattice parameter of $a_{200} = 3.987$ Å and $a_{200} = 3.764$ Å, respectively. By aging the solution-treated specimen at 400 °C for 20000 min, the α_1 and α_2 phases were transformed into the α_1' and α_2' phases of an f.c.c. structure with a lattice parameter of $a_{200} = 4.041$ Å and $a_{200} = 3.719$ Å, respectively. The Ag, Pd, Cu and Au elements which constitute the specimen alloy have an f.c.c. structure, and their lattice parameter is reported to be $a = 4.0863$ Å, $a = 3.8908$ Å, $a = 3.6148$ Å and $a = 4.0786$ Å, respectively [7]. Judging from the fact that the major element of specimen alloy is Ag which has a lattice parameter of $a = 4.0863$ Å, it is supposed

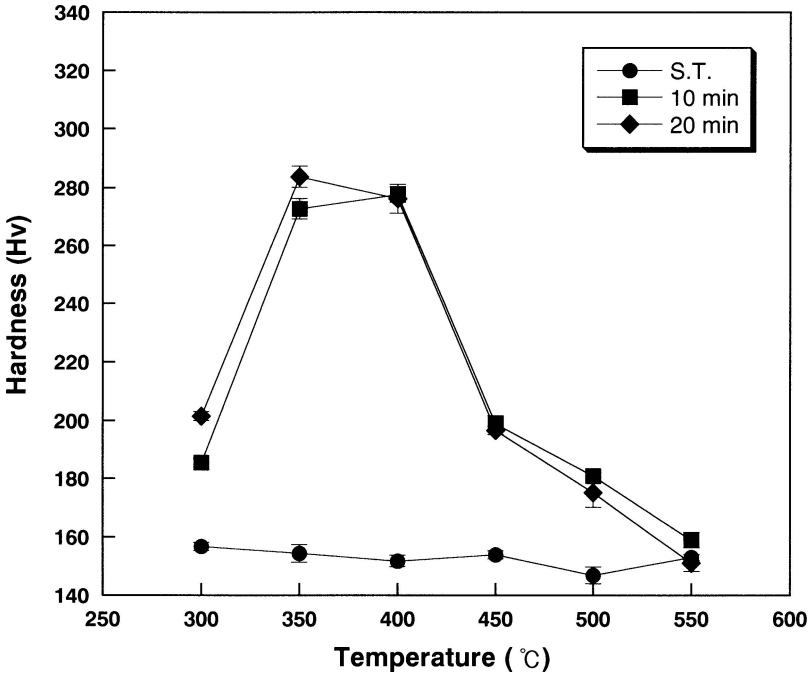

Figure 1 Isochronal age-hardening curves of the specimen alloy aged in the temperature ranges of 300 to 550 °C for 10 and 20 min.

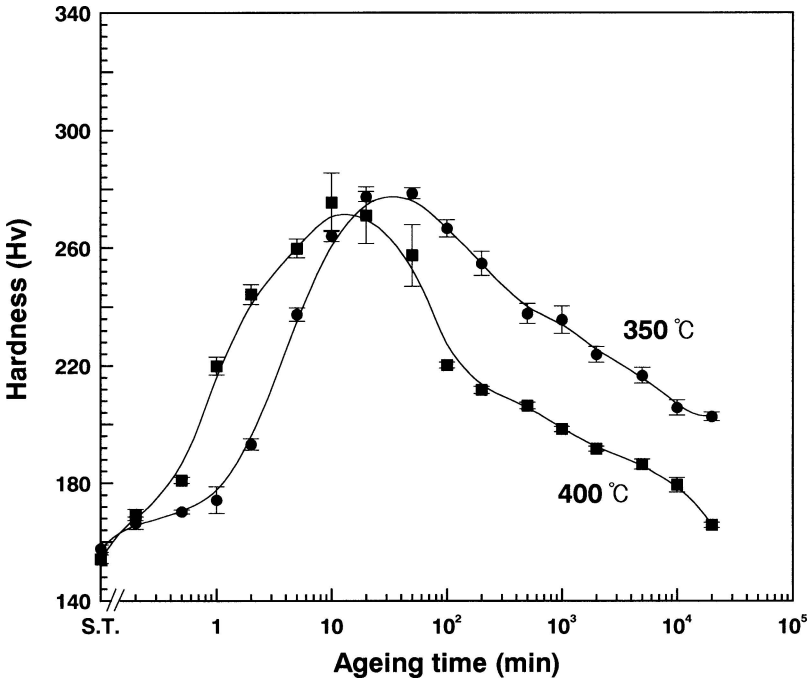

Figure 2 Isothermal age-hardening curves of the specimen alloy aged at 350 and 400 °C.

that the α_1 phase with stronger peak intensity and the product α_1' phase are based on the Ag-rich phase with a little difference in lattice parameter. Similarly, from the alloy composition and the lattice parameter, the α_2 phase with weaker peak intensity and the product α_2' phase are supposed to be based on the Cu-rich phase containing elements of relatively large atomic size. By the phase transformation of α_1 and α_2 into α_1' and α_2', the lattice parameters became close to those of Ag and Cu, respectively. The phase diagram of the Ag-Cu binary system shows that the equilibrium solubility of Cu in the Ag-rich phase and that of Ag in the Cu-rich phase at 400 °C is much less than that at 750 °C [8]. Therefore, the Cu atoms diffuse from the Ag-rich phase to the Cu-rich phase, while the Ag atoms diffuse in the opposite direction. Thus, it is thought that the changes in the lattice parameter are caused by the solubility limit of the Cu and Ag elements which contained in the α_1 and α_2 phases, respectively.

To understand the relation between the phase transformation and the hardness changes during the isothermal aging, the XRD changes of Fig. 3 and the age-hardening curves of Fig. 2 were considered together. Until the aging time of 5 min when the hardness increased apparently, the 111 peak intensity of the parent α_1 phase decreased drastically with the increase of that of the product α_1' phase at the lower diffraction angle. And without apparent changes in the 111 peak intensity

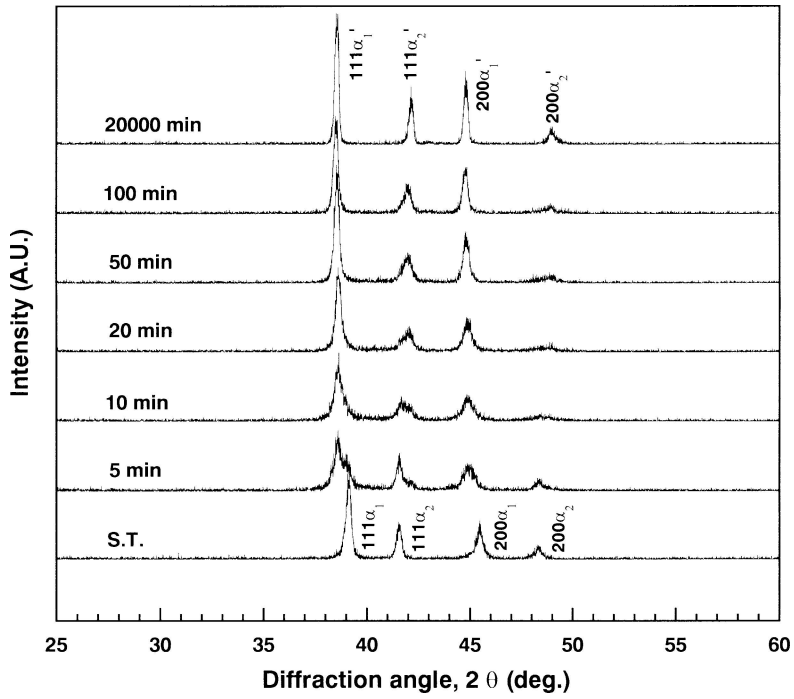

Figure 3 Variations of the XRD pattern during the isothermal aging at 400 °C with aging time.

of the α_2 phase, the 111 peak of the product α_2' phase appeared at the higher diffraction angle of that of the parent α_2 phase. From these facts, it is considered that the appearance of the 111 α_2' peak at the aging time of 5 min is caused by the diffusion of Cu from the Ag-rich α_1 phase, and that the increase in hardness is greatly related to the changes in the α_1 phase rather than that in the α_2 phase. At the aging time of 10 min when the maximum hardness value was obtained, the 111 peak of the parent α_1 phase was almost disappeared, while the 111 peak intensity of the parent α_2 phase was stronger than that of the product α_2' phase. The 111 peak intensity of the parent α_2 phase and the product α_2' phase was inversed at the aging time of 20 min when the maximum hardness value was maintained. During decrease in hardness, the 111 peak of the α_1' phase became sharp, and after that, the broad 111 peak of the α_2' phase became sharp finally.

In Fig. 3, the diffraction peaks broadened in the initial stage of phase transformation, and became sharp in the later stage of phase transformation. Such a broadening of the diffraction peaks during the phase transformation indicates the formation of coherency strains in the matrix [9, 10]. In the studies about the age-hardening mechanisms of dental alloys, it has been reported that the coherency strains which are formed in the matrix during the phase transformation cause the hardness increase in various dental alloys [11–14]. In the present study, the hardness increase in the early stage of the age-hardening process is supposed to be attributed to the coherency strains which are formed during the phase transformation of α_1 into α_1' rather than that of α_2 into α_2'. As can be seen in Fig. 3, the broad 111 α_1' peak grew sharp after the aging time of 10 min when the maximum hardness value was obtained. This means the release of coherency strains. However, the drastic decrease of hardness occurred after the aging time of 20 min. It is thought that the decrease of hardness was restrained for short periods of time by the coherency strains that formed during the early stage of phase transformation of α_2 into α_2' which occurred later than that of α_1 into α_1'.

3.3. Microstructural changes and element distribution

SEM observations were done to elucidate the microstructural changes during the phase transformation. Fig. 4 is showing the SEM photographs of 3000 (a), 5000 (b) and 15000 (c) magnifications for the specimens solution-treated at 750 °C for 30 min (1) and aged at 400 °C for 10 min (2) and 20000 min (3). In the SEM photographs of Fig. 4 (1), matrix, the lamellar structure and particle-like structures of various sizes were observed. To identify the element distribution of each structure, the EPMA analysis was done. Fig. 5 shows the distribution of Ag, Cu, Pd and Au in the specimen solution-treated at 750 °C for 30 min by the EPMA analysis. The matrix was distributed with the major component, Ag, of the specimen alloy, and the particle-like structures of various sizes were composed of mainly the Cu and Pd elements. The Au element was evenly distributed throughout the specimen. From the EPMA analysis and the XRD results, it can be said that the matrix is the Ag-rich α_1 phase containing small amounts of Au, and that the particle-like structures are the Cu-rich α_2 phase containing large amounts of Pd and small amounts of Au. The elements which constitute the lamellar structure could not be detected by the EPMA analysis because of the finer nature of the lamellar structure. However, from the fact that the XRD results of the solution-treated specimen show only two phases of the Ag-rich α_1 and Cu-rich α_2, it is thought that the lamellar structure is composed of the Ag-rich α_1 and Cu-rich α_2 phases.

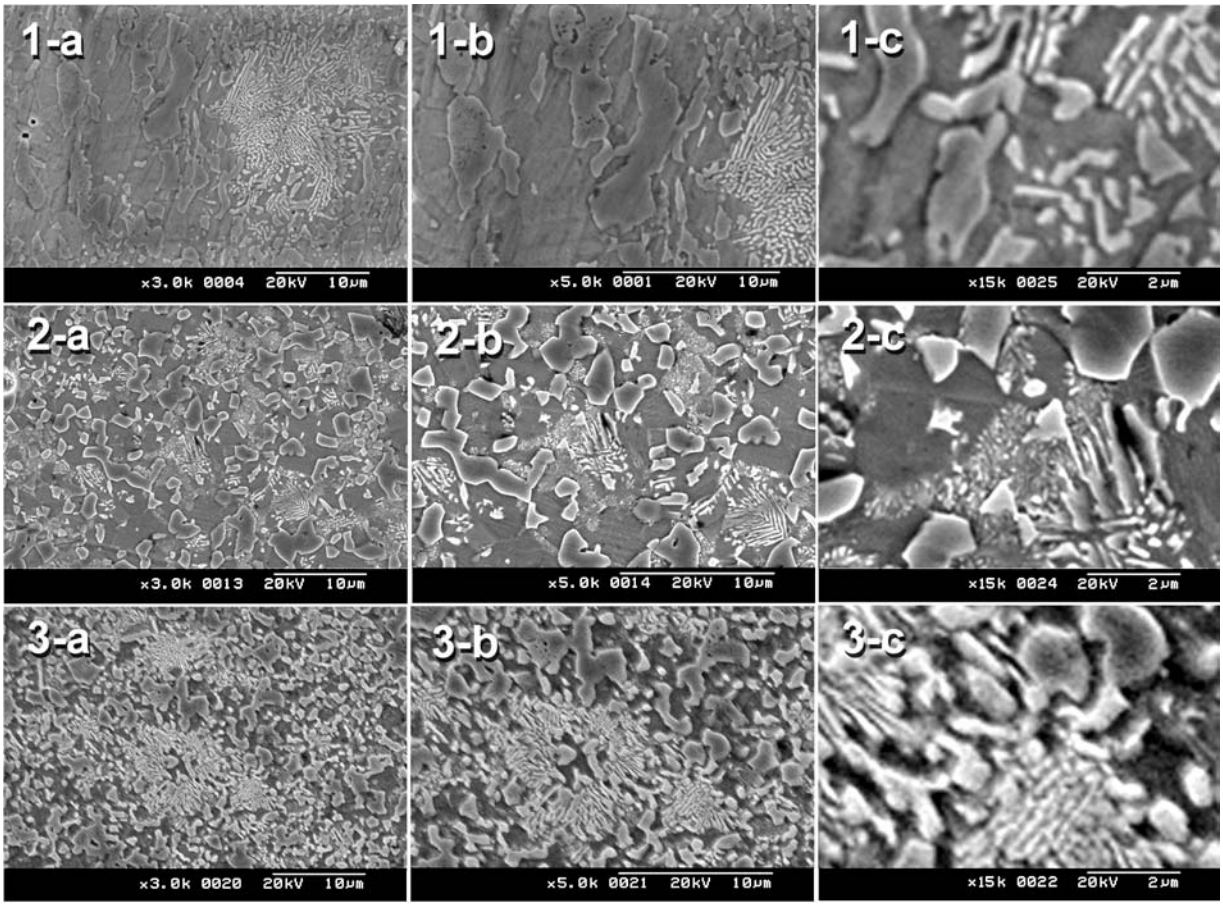

Figure 4 SEM photographs of 3000 (a), 5000 (b) and 15000 (c) magnifications for the specimens solution-treated at 750 °C for 30 min (1) and aged at 400 °C for 10 min (2) and 20000 min (3).

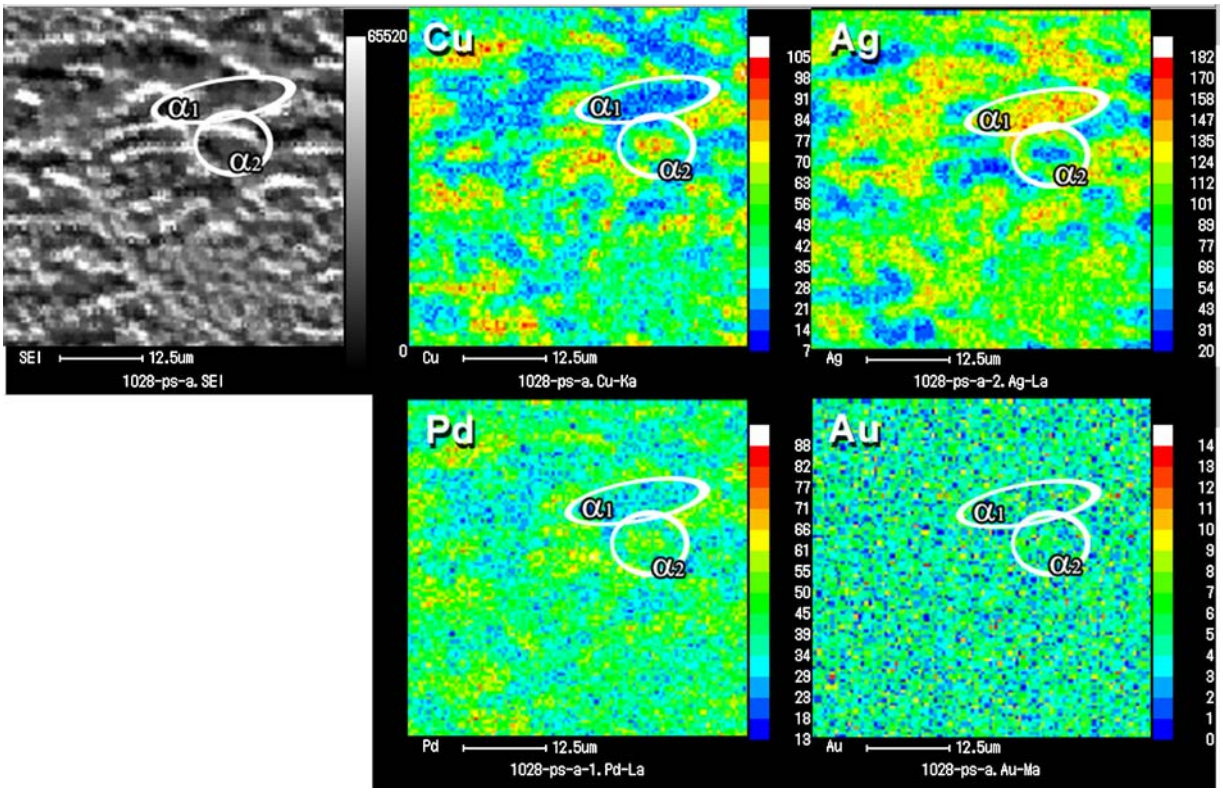

Figure 5 Element distribution in the specimen solution-treated at 750 °C for 30 min by the EPMA analysis.

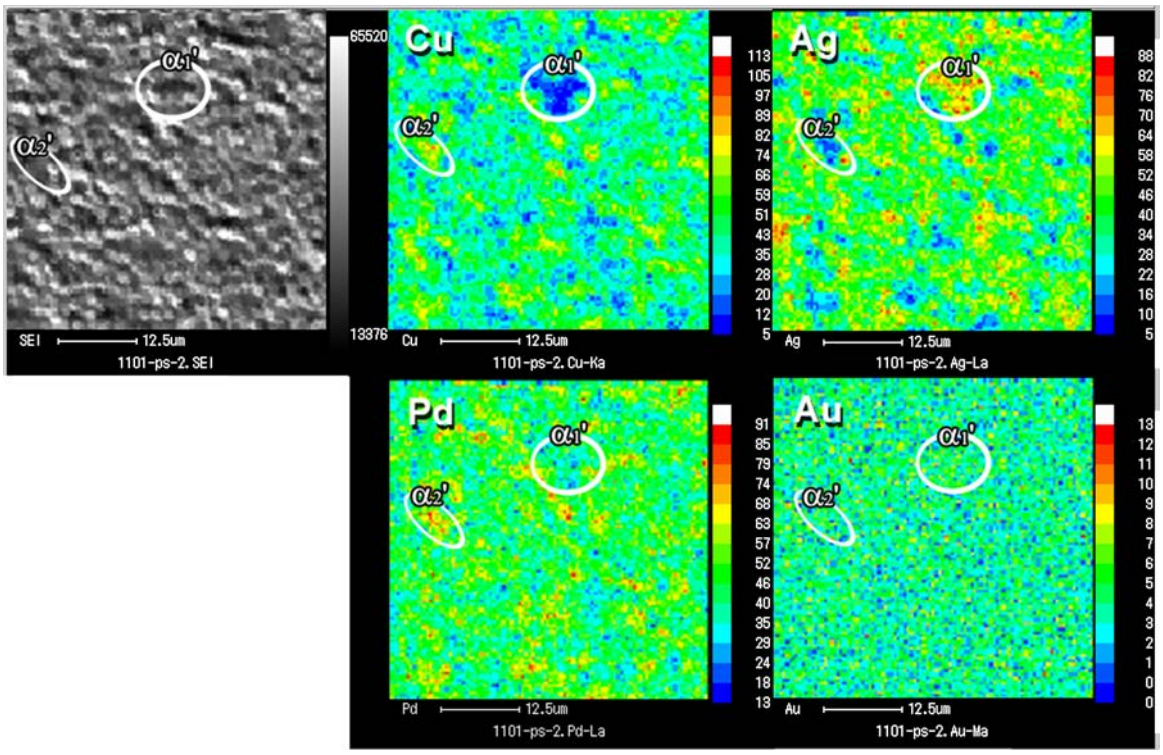

Figure 6 Element distribution in the specimen aged at 400 °C for 20000 min by the EPMA analysis.

SEM photographs of Fig. 4(2) shows the microstructure when the maximum hardness value was obtained by aging the specimen at 400 °C for 10 min. In Fig. 4(2), it was observed that very fine precipitates were newly formed in the matrix, which is much finer than the lamellar structure which is observed in the solution-treated specimen of Fig. 4(1). SEM photographs of Fig. 4(3) shows the microstructure when the hardness value decreased by aging the specimen at 400 °C for 20000 min. In Fig. 4(3), the very fine precipitates which were observed in Fig. 4(2) were grown and coarsened significantly. The changes of the lamellar structure and the particle-like structures were not clear compared to the changes in the matrix. Fig. 6 shows the EPMA analysis of the overaged specimen in which the precipitates were coarsened and covered the matrix by prolonged aging until 20000 min at 400 °C. The element distribution of the overaged specimen was similar to that of the solution-treated specimen of Fig. 5. The solute-depleted matrix and particle-like structures are composed of the Ag-rich α_1' phase and the Cu-rich α_2' phase containing Pd, respectively. The element distribution of the lamellar structure and precipitates could not be detected by the EPMA analysis because of the finer nature. Considering the XRD results which show that the lattice parameters became close to those of Ag and Cu by phase transformation of α_1 and α_2 into α_1' and α_2', it is thought that the appearance of precipitates in the Ag-rich matrix is caused by the diffusion and precipitation of the Cu element from the Ag-rich α_1 matrix during the aging at 400 °C. Thus, the fine precipitates are expected to be the Cu-rich α_2' phase. And the lamellar structure is thought to be composed of the α_1' and α_2' phases from the XRD results which are showing only two phases of the Ag-rich α_1' and Cu-rich α_2' for the overaged specimen. From above results, it is thought that the drastic increase in hardness is mainly attributed to the early stage of precipitation of the Cu-rich α_2' phase from the Ag-rich α_1 matrix. In the overaged specimen, the very fine precipitates were coarsened. It is well known that the coarsening of the microstructure results in the decrease of hardness by releasing the coherency strains [11, 15–16]. In the present study, it is considered that the coherency strains in the interface between the Cu-rich precipitates and the solute-depleted Ag-rich matrix were released as the coarsening of the Cu-rich precipitates progressed by further aging, and that the release of the coherency strains resulted in the decrease of hardness in the latter stage of the age-hardening process.

The age-hardenability and hardening mechanism in the present study are similar to those in our previous study for the commercial dental silver alloy composed of 55 wt% Ag −20.9 wt% Pd −8.5 wt% Cu −12.5 wt% Au [17]. However, the relatively high Cu content of the specimen alloy in the present study resulted in changes of the microstructure, that is, the appearance of the lamellar structure of the Ag-rich and Cu-rich phases, and the formation of the Cu-rich particle-like structures containing Pd instead of a CsCl-type, CuPd particle-like structures in the solution-treated state. Thus, it is thought that the Cu is indispensable to the age-hardenability of the silver alloys, but the Cu content of much more than solubility limit in the silver alloys does not have an effect on improvement of the age-hardenability. And it is considered that the relatively high Cu content in silver alloys must decrease the chemical stability of the alloys by forming complex eutectic microstructures, but most of the Cu elements in this silver alloy exist as chemically stable form to some extent by containing the Pd element.

4. Conclusion

The age-hardening behaviour and related microstructural changes of a silver alloy with relatively high Cu content was investigated and the following results were obtained.

1. The hardness of the solution-treated specimen began to increase and reached a maximum value with increasing aging time, and then the hardness decreased gradually after maintaining the maximum value for short periods of time.
2. The microstructure of the solution-treated specimen was composed of the Ag-rich matrix, the Cu-rich particle-like structures containing Pd, and the lamellar structure of both phases.
3. It seemed that the Cu element diffused and precipitated from the Ag-rich matrix by aging, and by further aging, the fine Cu-rich precipitates were grown and coarsened.
4. The early stage of precipitation of the Cu-rich phase from the Ag-rich matrix by the solubility limit seemed to have caused the increase in hardness. The decrease in hardness was attributed to the coarsening of the Cu-rich precipitates in the later stage of the age-hardening process.

References

1. R. OUCHIDA, T. SHIRAISHI, M. NAKAGAWA and M. OHTA, *J. Mater. Sci.* **30** (1995) 3863.
2. R. OUCHIDA, S. MATSUYA, T. SHIRAISHI, M. NAKAGAWA, M. OHTA and Y. TERADA, *J. Alloys Comp.* **292** (1999) 281.
3. T. KAINUMA and R. WATANABE, *J. Jpn. Inst. Metals.* **33** (1969) 198.
4. M. OHTA, K. HISATSUNE and M. YAMANE, *J. Less-Common Met.* **65** (1979)11.
5. M. OHTA, T. SHIRAISHI, K. HISATSUNE and M. YAMANE, *J. Dent. Res.* **59** (1980) 1966.
6. L. NIEMI and H. HERO, *J. Dent. Res.* **63** (1984) 149.
7. B.D. CULLITY, In "Elements of X-ray Diffraction", 2nd ed. (Addison-Wesley publishing Co., Inc., Massachusetts, 1978) p. 506.
8. T. B. MASSALSKI, In "Binary Alloy Phase Diagrams", 2nd ed. (ASM International, Materials Park, Ohio, 1990) p. 29.
9. Y. TANAKA, K. UDOH, K. HISATSUNE and K. YASUDA,*Materials Transactions, JIM.* **39** (1998) 87.
10. H. J. SEOL, T. SHIRAISHI, Y. TANAKA, E. MIURA and K. HISATSUNE, *J Mater. Sci. : Mater. Med.* **13** (2002) 237.
11. H. I. KIM, H. K. AHN, H. K. LEE, K. HISATSUNE, H. J. SEOL and Y. TAKUMA, *Dent. Mater. J.* **18** (1999) 314.
12. M. OHTA, T. SHIRAISHI, M. YAMANE and K. YASUDA, *ibid.* **2** (1983) 10.
13. H.J. SEOL, T. SHIRAISHI, Y. TANAKA, E. MIURA, K. HISATSUNE and H.I. KIM, *Biomaterials.* **23** (2002) 4873.
14. K. YASUDA, *Gold Bull.* **20** (1987) 90.
15. H.I. KIM, M.I. JANG, M.S. KIM, *J. Oral. Rehabil.* **26** (1999) 215.
16. H.K. LEE, H.M. MOON, H.J. SEOL, J.E. LEE, H.I. KIM, *Biomaterials.* **25** (2004) 3869.
17. H.J. SEOL, G.C. KIM, K.H. SON, Y.H. KWON and H.I. KIM, *J. Alloys Comp.* **387** (2005) 139.

Received 2 May
and accepted 10 June 2005